Eur. Phys. J. A **22**, 337–345 (2004)
DOI 10.1140/epja/i2003-10235-7

THE EUROPEAN PHYSICAL JOURNAL A

Equation of state of nuclear matter and neutron stars in a hadron mass scaling frame

B. Liu[1], H. Guo[2], V. Greco[3,4], U. Lombardo[3], M. Di Toro[3,a], and Cai-Dian Lü[1]

[1] Institute of High Energy Physics, Chinese Academy of Sciences, Beijing 100039, PRC
[2] Department of Technical Physics, Peking University, Beijing 100871, PRC
[3] Laboratori Nazionali del Sud, via S. Sofia 44, I-95123 Catania and University of Catania, Catania, Italy
[4] Cyclotron Institute, Texas A & M University, College Station, TX, USA

Received: 24 November 2003 / Revised version: 29 April 2004 /
Published online: 3 November 2004 – © Società Italiana di Fisica / Springer-Verlag 2004
Communicated by A. Molinari

Abstract. The equation of state for nuclear matter at finite temperature and the properties of neutron stars are studied starting from an effective Lagrangian in the framework of the relativistic mean field theory. We find that the empirical properties of nuclear matter can be reproduced if the medium effects are mainly described in terms of the Brown-Rho mass scaling on top of the Bonn potential used as the underlying bare nucleon-nucleon interaction. In particular a correct symmetry energy at saturation density is obtained. The extrapolation of the equation of state to neutron matter and some predictions for the neutron-star masses are finally discussed and compared with other nucleonic many-body approaches.

PACS. 21.65.+f Nuclear matter – 21.30.Fe Forces in hadronic systems and effective interactions – 97.60.Jd Neutron stars

1 Introduction

The understanding of the properties of nuclear matter under extreme conditions is a crucial and indispensable goal of nuclear physics and astrophysics. In particular, the study of asymmetric nuclear matter and neutron stars remains an important motivation for building the radioactive ion beam facilities. The extraction of information on the equation of state (EOS) for dense matter from collision data as well as from astrophysical observations represents a strong check for the existing nuclear matter models.

The Walecka model [1,2], based on the relativistic mean-field (RMF) theory, and its extensions, which include nonlinear meson interactions [3,4] and derivative scalar couplings [5], have been successfully used to study the properties of nuclear and neutron matter, β-stable nuclei and extended to the drip-line region. The RMF approach has also been intensively used to study the nuclear matter under extreme conditions of temperature, density and isospin asymmetry with the purpose of describing neutron stars and supernova explosions.

Brown and Rho have developed a type of density-dependent effective field theory in nuclear matter based on chiral-symmetry requirements [6]. The in-medium masses of hadrons (baryons and mesons) have to be modified in order to guarantee the partial restoration of the chiral symmetry predicted by QCD in the nuclear medium. Experimental evidence for that is believed to be the anomalous lepton production observed in the invariant mass region around 400 MeV in heavy-ion collisions performed by $CERES$ [7] and $HELIOS$ [8] Collaborations. Brown and Rho suggest to describe the effect of the nuclear medium on hadron masses by means of simple scaling laws, referred to as the Brown-Rho (BR) mass scaling laws [6]. The EOS of nuclear matter is a suitable benchmark to investigate the medium modifications of hadron properties, including the BR scaling. Aim of this work is to show that in fact the mass scaling is able to reproduce the main in-medium correlation effects on the nucleon-nucleon (NN) interaction.

An effective Lagrangian for nuclear matter was proposed in refs. [9–11] to study the in-medium effects described by the BR scaling. After the model parameters are calibrated by the properties of nuclear matter at the saturation density, this model can give reasonable results for symmetric nuclear matter at $T = 0$ MeV. However, the meson parameters (masses and coupling constants) along with other model parameters, are fixed completely by the empirical properties of nuclear matter at the saturation point so that the role played by the BR scaling turns out to be obscure as far as the in-medium modification of the NN interaction is concerned. Moreover in our scheme the clear separation of different in medium

[a] e-mail: ditoro@lns.infn.it

contributions, BR scaling *vs.* self-coupling terms, will also allow a check of the intrinsic consistency of the model, as discussed in sect. 3.

More appropriate to the scope is the attitude adopted by microscopic approaches. The effective interaction, which is supposed to reproduce the saturation properties of nuclear matter, also reduces to the basic NN interaction in the limit of vanishing baryonic density. On the other hand, the underlying NN interaction must be fixed by the experimental data on the two-body interaction in the vacuum, which is the case with realistic NN interactions such as Paris, Argonne or Bonn potentials. A few nuclear matter calculations, based on microscopic many-body approaches, such as Brueckner [12] and Dirac-Brueckner [13] theories, have proved that BR mass scalings can substantially contribute to reproduce the empirical saturation properties. In this work we will get similar results within the much simpler effective field framework (RMF), easier to apply to nuclear structure and dynamics problems.

The in-medium effective Lagrangian describing the interaction between nucleons and mesons should be then expressed in terms of parameters which, in the limit of zero density, are consistent with the experimental phase shifts of the free NN scattering and with deuteron binding energy. The parameters, bare meson masses and coupling constants, of the Bonn potential [14] are quite suitable for such a purpose. They fulfill the above-mentioned experimental constraints and have been extensively used in microscopic calculations of nuclear matter. Therefore, following the main task of this work, we construct the effective Lagrangian density just using the meson parameters from the Bonn potential, in particular the Bonn B potential, and impose on the baryon and meson mass the BR mass scaling.

Since the present approach is a mean-field approximation, it will be in any case necessary to introduce also nonlinear terms which take into account other many body correlation effects. The corresponding parameters are adjusted together with the scaling parameter to fit the empirical saturation density and energy of nuclear matter at zero temperature. The procedure appears to be consistent with convergence requirements for the nonlinear contributions. This result indicates that Fock, retardation and other correlations must be in any case introduced on top of the mass scaling. We will see that no further adjustment is required to get realistic values of the symmetry energy at saturation density for asymmetric matter. In any case, consistently with the philosophy of the paper, the bare *NN-Bonn* Lagrangian is recovered in the zero-density limit.

In this context we study the nuclear EOS at zero and finite temperature for different scaling parameters. We extend the calculation to isospin asymmetric nuclear matter also in order to investigate the implications of our EOS for neutron-stars.

The main conclusion is that such relatively simple procedure to get a functional form of the nucleonic energy density appears to be valid in a wide range of baryon densities, from the description of the liquid-gas phase transition of very dilute matter to a reasonable prediction of neutron star properties.

The paper is organized as follows. In sect. 2, the model with the BR scaling is presented. The nuclear equation of state at finite temperature is given in sect. 3. The nuclear symmetry energy and the β-equilibrium nuclear matter are presented in sects. 4 and 5, respectively. The properties of neutron stars are given in sect. 6. General comments and a summary of main conclusions are presented in sect. 7.

2 The model

The starting point is the relativistic Lagrangian density with the BR mass scaling

$$\begin{aligned}\mathcal{L} = &\bar{\psi}[i\gamma_\mu\partial^\mu - M^\star + g_\sigma\phi - g_\omega\gamma_\mu\omega^\mu - g_\rho\gamma^\mu\vec{\tau}\cdot\vec{b}_\mu]\psi \\ &+\frac{1}{2}(\partial_\mu\phi\partial^\mu\phi - m_\sigma^{\star 2}\phi^2) - U(\phi) \\ &+\frac{1}{2}m_\omega^{\star 2}\omega_\mu\omega^\mu + \frac{1}{4}c(\omega_\mu\omega^\mu)^2 \\ &+\frac{1}{2}m_\rho^{\star 2}\vec{b}_\mu\cdot\vec{b}^\mu \\ &-\frac{1}{4}F_{\mu\nu}F^{\mu\nu} - \frac{1}{4}\vec{G}_{\mu\nu}\vec{G}^{\mu\nu} \quad ,\end{aligned} \tag{1}$$

where ϕ, ω_μ, and $\vec{b}_\mu$ stand for the σ-, ω-, and ρ-meson fields, $\vec{\tau}$ is for the isospin matrix, $F_{\mu\nu} = \partial_\mu\omega_\nu - \partial_\nu\omega_\mu$, $\vec{G}_{\mu\nu} = \partial_\mu\vec{b}_\nu - \partial_\nu\vec{b}_\mu$, and c is the parameter of a nonlinear potential of ω-meson. A nonlinear potential of σ-meson is denoted as

$$U(\phi) = \frac{1}{3}a\phi^3 + \frac{1}{4}b\phi^4 \quad , \tag{2}$$

where a and b are the parameters of the potential. The hadron masses are scaled according to the BR scaling laws

$$\frac{M^\star}{M} = \frac{m_\sigma^\star}{m_\sigma} = \frac{m_\omega^\star}{m_\omega} = \frac{m_\rho^\star}{m_\rho} = \Phi(\rho) \quad . \tag{3}$$

The scaling function is assumed to be [9–11]

$$\Phi(\rho) = \frac{1}{1 + y\rho/\rho_0} \quad , \tag{4}$$

where y is the scaling parameter.

Since the Lagrangian density, eq. (1), is density-dependent, rearrangement contributions arise in the equation of motion for the baryon field. One obtains [10]

$$\begin{aligned}\frac{\partial\mathcal{L}}{\partial\bar{\psi}} &= \frac{\partial\mathcal{L}}{\partial\bar{\psi}} + \frac{\partial\mathcal{L}}{\partial\hat{\rho}}\frac{\partial\hat{\rho}}{\partial\bar{\psi}} \\ &= (i\gamma_\mu\partial^\mu - M^\star + g_\sigma\phi - g_\omega\gamma_\mu\omega^\mu \\ &\quad -g_\rho\gamma^\mu\vec{\tau}\cdot\vec{b}_\mu + u_\mu\gamma^\mu\Sigma)\psi = 0 \ ,\end{aligned} \tag{5}$$

where the rearrangement self-energy Σ is

$$\begin{aligned}\Sigma = \frac{\partial\mathcal{L}}{\partial\hat{\rho}} &= m_\omega^\star\omega_\mu\omega^\mu(\frac{\partial m_\omega^\star}{\partial\hat{\rho}}) + m_\rho^\star\vec{b}_\mu\cdot\vec{b}^\mu(\frac{\partial m_\rho^\star}{\partial\hat{\rho}}) \\ &\quad -m_\sigma^\star\phi^2(\frac{\partial m_\sigma^\star}{\partial\hat{\rho}}) - \bar{\psi}\psi\frac{\partial M^\star}{\partial\hat{\rho}} \ ,\end{aligned} \tag{6}$$

as done in ref. [9]. The following definitions have been adopted: $\hat{\rho}^2 = j_\mu j^\mu$ with $j_\mu = \bar{\psi}\gamma_\mu\psi$ and $u_\mu = \frac{1}{\sqrt{1-\vec{v}^2}}(1,\vec{v}) = \frac{1}{\sqrt{\rho^2-\vec{j}^2}}(\rho,\vec{j})$. $\vec{j} = \langle\bar{\psi}\vec{\gamma}\psi\rangle$ (baryon current density), and $\rho = \langle\psi^+\psi\rangle$ (baryon density).

In the mean-field approximation (MFA, see [9]), Σ_0 is given by

$$\Sigma_0 = \langle\Sigma\rangle|_{\vec{v}=0} = m^\star_\omega\omega_0^2\frac{\partial m^\star_\omega}{\partial\rho} + m^\star_\rho b_0^2\frac{\partial m^\star_\rho}{\partial\rho} - m^\star_\sigma\phi^2\frac{\partial m^\star_\sigma}{\partial\rho} - \langle\bar{\psi}\psi\rangle\frac{\partial M^\star}{\partial\rho}\ . \tag{7}$$

The equations of motion for baryon and meson fields with the BR mass scaling in MFA are

$$\begin{aligned}&(i\gamma_\mu\partial^\mu - M^\star + g_\sigma\phi - g_\omega\gamma^0\omega_0 - g_\rho\gamma^0\tau_3 b_0 + \gamma^0\Sigma_0)\psi = 0\\ &m^{\star 2}_\sigma\phi + a\phi^2 + b\phi^3 = g_\sigma\langle\bar{\psi}\psi\rangle = g_\sigma\rho_{\rm s}\\ &(m^{\star 2}_\omega + c\omega_0^2)\omega_0 = g_\omega\langle\psi^+\psi\rangle = g_\omega\rho\\ &m^{\star 2}_\rho b_0 = g_\rho\langle\psi^+\tau_3\psi\rangle = g_\rho\rho_3\ ,\end{aligned} \tag{8}$$

where $\rho_3 = \rho_p - \rho_n$, ρ and $\rho_{\rm s}$ are the baryon and the scalar densities, respectively.

Neglecting the derivatives with respect to meson fields, the energy-momentum tensor can be written as

$$T_{\mu\nu} = i\bar{\psi}\gamma_\mu\partial_\nu\psi + [\frac{1}{2}m^{\star 2}_\sigma\phi^2 + U(\phi) - \frac{1}{2}m^{\star 2}_\omega\omega_\lambda\omega^\lambda - \frac{1}{4}c(\omega_\lambda\omega^\lambda)^2 - \frac{1}{2}m^{\star 2}_\rho\vec{b}_\lambda\vec{b}^\lambda + \bar{\psi}u_\lambda\gamma^\lambda\Sigma\psi]g_{\mu\nu}\ , \tag{9}$$

with $u_\mu = (1,\vec{0})$ in the rest frame.

3 Nuclear equation of state at finite temperature

The properties of nuclear matter at finite temperature are described by the thermodynamic potential: $\Omega = -pV = -\frac{1}{\beta}\ln Z$, where β is the inverse of temperature, $\beta = 1/k_{\rm B}T$, and Z is the grand partition function given by $Z = {\rm Tr}[e^{-\beta(\hat{H}-\Sigma_i(\mu_i\hat{B}_i))}]$. $\hat{H}$ is the Hamiltonian operator, $\hat{B}_i$ is the baryon number operator for neutron ($i = n$) and proton ($i = p$), μ_i is the chemical potential. The nuclear EOS with the BR mass scaling at finite temperature is obtained from the thermodynamic potential Ω as [2]

$$\epsilon = \sum_{i=n,p} 2\int\frac{{\rm d}^3k}{(2\pi)^3}E^\star_N(k)(n_i(k)+\bar{n}_i(k)) + \frac{1}{2}m^{\star 2}_\sigma\phi^2 + U(\phi) + \frac{1}{2}m^{\star 2}_\omega\omega_0^2 + \frac{3}{4}c\omega_0^4 + \frac{1}{2}m^{\star 2}_\rho b_0^2\ , \tag{10}$$

$$P = \sum_{i=n,p}\frac{2}{3}\int\frac{{\rm d}^3k}{(2\pi)^3}\frac{k^2}{E^\star_N(k)}(n_i(k)+\bar{n}_i(k)) - \frac{1}{2}m^{\star 2}_\sigma\phi^2 - U(\phi) + \frac{1}{2}m^{\star 2}_\omega\omega_0^2 + \frac{1}{4}c\omega_0^4 + \frac{1}{2}m^{\star 2}_\rho b_0^2 - \Sigma_0\rho\ , \tag{11}$$

Table 1. Parameters and coupling constants of Bonn-B potential [14], masses of nucleon and mesons are given in unit of MeV.

M	m_σ	m_ω	m_ρ	$g_\sigma^2/4\pi$	$g_\omega^2/4\pi$	$g_\rho^2/4\pi$
939	550	782.6	769	8.0769	20	0.95

where $E^\star_N = \sqrt{k^2 + M^{\star\,2}_N}$, the effective mass $M^\star_N$ is defined as $M^\star_N = M^\star - g_\sigma\phi$, here $M^\star$ is the BR scaling mass of the nucleon given in eq. (3). The $n_i(k)$ and $\bar{n}_i(k)$ in eqs. (10) and (11) are the fermion and antifermion distribution functions

$$n_i(k) = \frac{1}{1+\exp\{(E^\star_N(k)-\mu^\star_i)/k_{\rm B}T\}}\ , \tag{12}$$

and

$$\bar{n}_i(k) = \frac{1}{1+\exp\{(E^\star_N(k)+\mu^\star_i)/k_{\rm B}T\}}\ , \tag{13}$$

where the effective chemical potential $\mu^\star_i$ is determined by the nucleon density ρ_i

$$\rho_i = 2\int\frac{{\rm d}^3k}{(2\pi)^3}(n_i(k)-\bar{n}_i(k))\ , \tag{14}$$

and the $\mu^\star_i$ is related to the chemical potential μ_i of neutron ($i = n, (+)$) and proton ($i = p, (-)$) by the equation

$$\mu^\star_i = \mu_i - g_\omega\omega_0 + \Sigma_0 \mp g_\rho b_0\ . \tag{15}$$

The scalar density $\rho_{\rm s}$ is given by

$$\rho_{\rm s} = 2\sum_{i=n,p}\int\frac{{\rm d}^3k}{(2\pi)^3}\frac{M^\star_N}{E^\star_N}(n(k)+\bar{n}(k))\ . \tag{16}$$

For the asymmetric nuclear matter, one introduces the asymmetry parameter α, which is defined as $\alpha = (\rho_n - \rho_p)/\rho$ with $\rho_n = \frac{1+\alpha}{2}\rho$ and $\rho_p = \frac{1-\alpha}{2}\rho$. Obviously, the nuclear EOS is a function of baryon density ρ, temperature T and asymmetry parameter α. Thus, the energy density and pressure for symmetric and asymmetric nuclear matter at finite temperature can be self-consistently calculated from eqs. (10) and (11).

In the present model, the hadronic masses and the coupling constants from the Bonn-B potential are listed in table 1. The binding energy is defined by $E/A = \epsilon/\rho - M$. As pointed out in ref. [15], the spin-orbit splittings in finite nuclei are approximately connected to the properties of nuclear matter, in particular to the nucleon effective mass. The suggested value of $M^\star_N = 0.60M$ at the saturation point of nuclear matter ρ_0=0.16 fm^{-3}, with a binding energy $E/A = -16$ MeV, is taken to be as our input. Then, the coefficients of the σ- and ω-meson self-interaction terms, $A = a/g_\sigma^3$, $B = b/g_\sigma^4$ and $C = c/g_\omega^4$, are determined by adjusting the scaling parameter y. The obtained coefficients for different values of y are presented in table 2.

Table 2. Model parameters.

y	A (fm^{-1})	B	C	K (MeV)
0.10	−0.0230298	0.0337494	0.0096414	192
0.08	−0.0300563	0.0324686	0.0102347	231
0.06	−0.0354435	0.0306952	0.0111201	276
0.00	−0.0434008	0.0235143	0.0181230	484

In the same table the corresponding numerical results for the nuclear matter incompressibility $K = 9\frac{\partial P}{\partial \rho}|_{\rho=\rho_0}$, for symmetric matter, are also reported.

We see that the incompressibility of nuclear matter increases as y decreases, in spite of the nonlinear term corrections. The value of K at $y = 0$ is 484 MeV, which seems too large in comparison with the empirical estimations [5]. On the other hand if the nonlinear potentials for σ and ω mesons vanish in the present model, *i.e.* $a = b = c = 0$, our numerical calculations indicate that it is impossible to get reasonable saturation properties of nuclear matter with *and* without the BR mass scaling. Therefore, the nonlinear potentials of σ and ω mesons are certainly important. A nice feature of our approach is that we are able to saparate the various contributions from in medium effects. In the following we will quantitatively analyze the interplay between self-interacting terms and BR scaling for the effective mass determination.

In contrast, in previous studies along the same line, see ref. [10], two scaling parameters are introduced while all the other model parameters still need to be fully fitted at the saturation point of nuclear matter. In this way the link to the bare interaction disappears.

Since the behavior of the nuclear EOS given by the three sets of parameters with the BR mass scaling in table 2 is similar, we only present the results obtained with the scaling parameter $y = 0.10$.

3.1 Nucleon effective masses

The comparison between the BR scaled mass $M^\star$ and the effective nucleon mass $M_N^\star$ with $y = 0.10$ is displayed in fig. 1. Both masses are decreasing with increasing density, and the difference between $M^\star$ and $M_N^\star$ becomes considerable large in the high-density region. It should be noted that the attractive interaction stemmed from the σ-meson exchange mainly leads to the decrease of the effective nucleon mass. Moreover we have superimposed in-medium effects described by the decrease of the BR scaling mass coupled to the self-coupling contributions. A more detailed analysis on the weight of the different terms at saturation can be useful to better understand the structure of the model.

Starting from an approximated estimation of the scalar density at saturation

$$\rho_{0\mathrm{s}} \simeq \rho_0 \frac{M_N^\star}{\sqrt{k_\mathrm{F}^2 + {M_N^\star}^2}} = 0.13\,\mathrm{fm}^{-3},$$

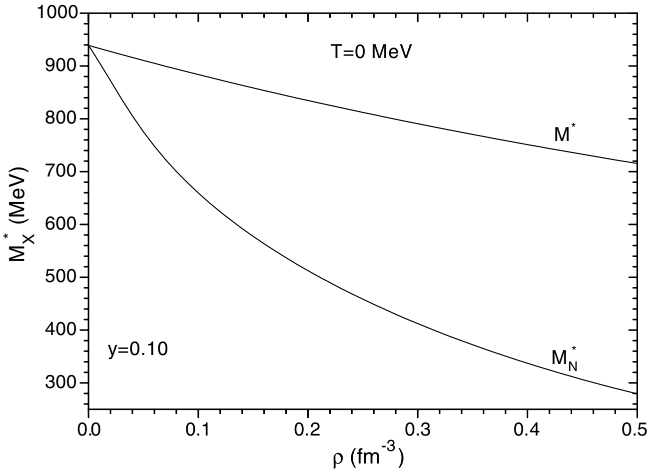

Fig. 1. Comparison between the BR scaling mass $M^\star$ and the effective nucleon mass $M_N^\star$ as a function of the baryon density by the $y = 0.10$ set.

using a $M_N^\star \simeq 0.6 M_N$, we can get three different evaluations of the nucleon masses at ρ_0:

- Contribution of only the *linear-σ* part, without BR and non-linear terms. Using the free Bonn-B values of table 1 we have

$$f_\sigma \equiv \left(\frac{g_\sigma}{m_\sigma}\right)^2 = 13.04\,\mathrm{fm}^2$$

  and so an effective mass at saturation

$$M_N^\star = M - f_\sigma \rho_{0\mathrm{s}} = 604\,\mathrm{MeV}.$$

- Contribution of the BR scaling *only*, all masses scaled following the eq. (3) prescription with scaling parameter $y = 0.1$:

$$M_N^\star = M^\star(\mathrm{BR}) - \mathrm{f}_\sigma(\mathrm{BR})\rho_{0\mathrm{s}} = 456\,\mathrm{MeV}$$

  since $M^\star(\mathrm{BR}) = 853\,\mathrm{MeV}$ and the $f_\sigma(\mathrm{BR})$ coupling will increase to $15.75\,\mathrm{fm}^2$.
- Inclusion of also the self-coupling terms. We get the value of the complete calculation shown in fig. 1, *i.e.* $M_N^\star = 564\,\mathrm{MeV}$.

We can conclude that the corrections to the nucleon free mass are in this order:

linear only: $\Delta M(\mathrm{Lin}) = -334\,\mathrm{MeV}$,

adding the BR scaling: $\Delta M(\mathrm{BR}) = -148\,\mathrm{MeV}$,

adding the non-linear terms: $\Delta M(\mathrm{Nonlin}) = +108\,\mathrm{MeV}$.

The relative weights are roughly in the order 3 to 1.5 to 1. This nicely shows that the self-coupling contributions are still important. Moreover, it should be noted that the non linear terms effect is rapidly decreasing at low density as we can see from the structure of the eqs. (8). This is consistent with the general philosophy of this work, to recover the free-space *NN-Bonn* Lagrangian in the zero-density limit.

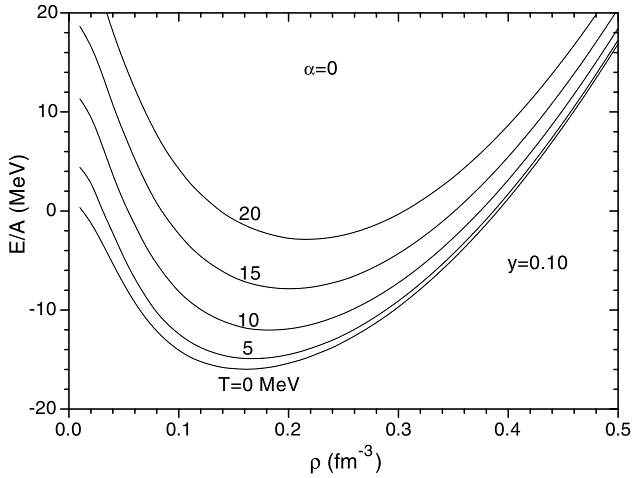

Fig. 2. Energy per nucleon as a function of the baryon density for symmetric nuclear matter ($\alpha = 0$) at different temperatures ($y = 0.10$ set).

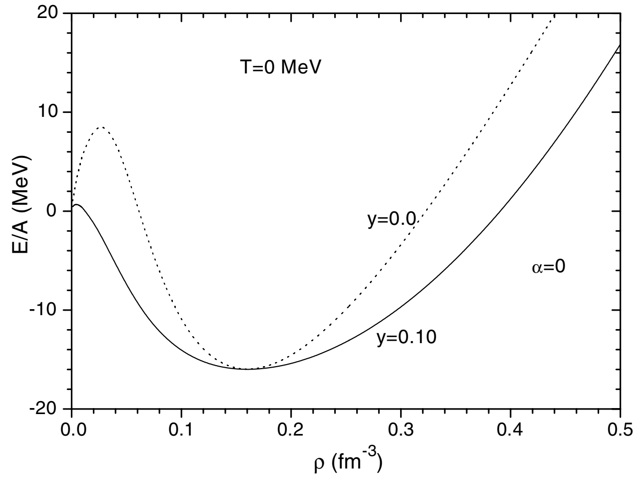

Fig. 4. Energy per nucleon as a function of the baryon density at $T = 0$ MeV by the $y = 0.0$ and 0.10 sets.

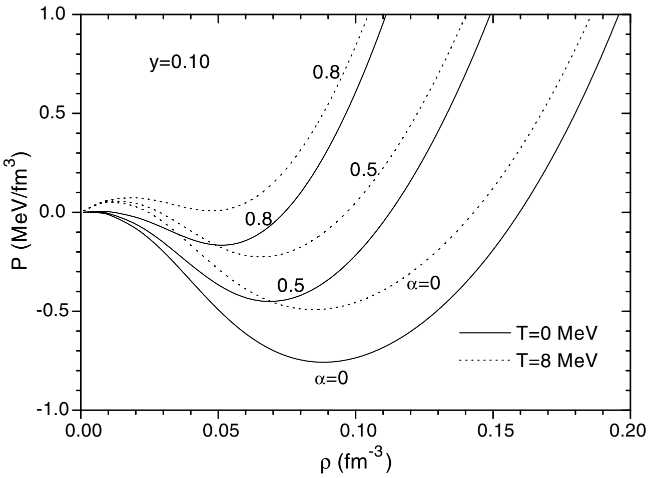

Fig. 3. Pressure as a function of the baryon density at $T = 0$ and 8 MeV for different α.

3.2 Phase diagram of nuclear matter

Figure 2 shows the energy per nucleon as a function of the baryon density for symmetric nuclear matter ($\alpha = 0$) with the $y = 0.10$ set at different temperatures. The results show that the increasing of temperature moves the curves upward, and makes the nuclear matter less bound. From the critical condition for the liquid-gas phase transition $\frac{\partial P}{\partial \rho}|_{T_c} = \frac{\partial^2 P}{\partial^2 \rho}|_{T_c} = 0$, we find the critical temperature $T_c = 18.63$ MeV in the present model. This critical temperature is comparable with that obtained by microscopic many-body calculations [16].

The pressure as a function of the baryon density at $T = 0$ and 8 MeV for different α with the $y = 0.10$ set is shown in fig. 3. The local minimum for a fixed T is shifted to the low-density region as α increases. The new equilibrium density, zero-pressure point, is also shifted to lower values, typical of a *stiff* symmetry energy, see refs. [17,18], as we will discuss in the following.

The pressure for a fixed α increases with increasing temperature. The local maximum at the low-density region for a fixed α is moved to the large-density region as temperature increases.

In order to compare the results with (solid line) and without (dotted line) the BR mass scaling, we plot the energy per nucleon as a function of the baryon density for symmetric nuclear matter at $T = 0$ MeV in fig. 4. The obtained results show that the behavior of the EOS without the BR mass scaling is not reasonable, especially in the low-density region; moreover, the incompressibility for nuclear matter turns out to be too large (also see table 2). The results illustrate that the BR mass scaling is quite necessary if the empirical properties of nuclear matter are to be reproduced starting from the Bonn potential parameters. The results in the present model with the BR mass scaling also show that the behavior of EOS for nuclear matter at finite temperature is consistent with that given by other more phenomenological RMF models [18–20]. We can conclude that within the above prescriptions the Bonn potential works well for nuclear matter in the framework of the RMF approximation.

4 Nuclear symmetry energy

One basic property of asymmetric nuclear matter for studying the structure of neutron stars is the density dependence of the nuclear symmetry energy $E_{\rm sym}(\rho)$. The latter is defined through the expansion of the binding energy in terms of the asymmetry parameter α

$$E/A(\rho,\alpha) = E/A(\rho,0) + E_{\rm sym}(\rho)\alpha^2 + O(\alpha^4) + \dots \quad (17)$$

Empirically, we have information on $E_{\rm sym}(\rho)$ only at the saturation point, where it ranges from 28 to 35 MeV according to the nuclear mass table [21].

It is well known that the symmetry energy has a kinetic contribution, from the different neutron/proton occupation of momentum space, and a interaction one, *e.g.*

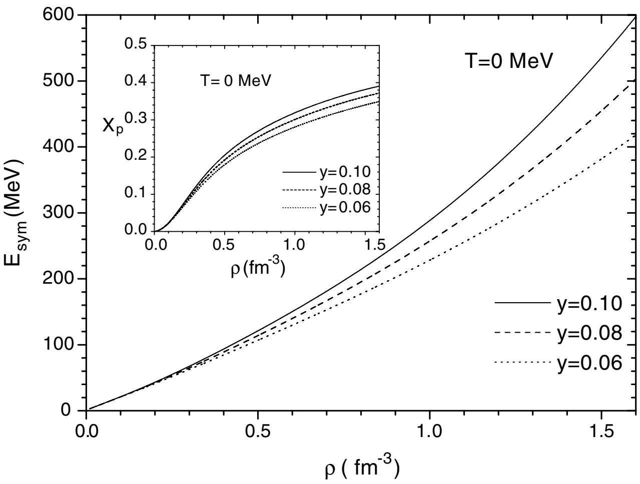

Fig. 5. Nuclear symmetry energy and proton fraction as a function of the baryon density at $T = 0\,\text{MeV}$ by different y sets.

see ref. [18]. The first is depending on nucleon effective masses which are actually fixed by saturation properties of symmetric matter (see sect. 3 before). The interaction part in our model is due to the ρ-meson coupling which is also fixed, see eqs. (3), (4), once the scaling parameter y is chosen, again from properties of symmetric matter. In this sense our estimation of the symmetry energy is deduced *without additional adjusted parameters*. Our evaluation of $E_{\text{sym}}(\rho_0)$ at saturation, the a_4 parameter of the Weiszaecker formula, obtained from extending the RMF calculation at finite isospin, is 34.0, 33.6 *and* 33.1 MeV for $y = 0.10$, 0.08 *and* 0.06, respectively, in the correct empirical range.

At this point we can extend our study to a predicted behavior in regions off saturation. We have then calculated $E_{\text{sym}}(\rho)$ in a range of densities relevant for applications in neutron stars. The results are plotted in fig. 5 for the three different scaling parameters. One main feature is that $E_{\text{sym}}(\rho)$ is monotonically increasing with density, the *stiff* behavior noted before, and reaches the critical threshold for direct $URCA$ processes to occur at rather low densities, of large interest for the neutron star cooling [22]. A way to probe the symmetry energy *vs.* density is that of determining the chemical composition of neutron stars in the β-equilibrium regime and the related structure properties, like the mass-radius correlation.

5 β-equilibrium nuclear matter at $\mathbf{T = 0}$

The β-equilibrium nuclear matter is relevant for the composition of the neutron star matter. In the present study we limit the constituents of a neutron star to be neutrons, protons and electrons. The aim of our discussion is indeed to compare with other microscopic many-body calculations at the same level of considering only nucleonic degrees of freedom.

The composition of neutron star matter is determined by the request of charge neutrality and equilibrium. The (n, p, e^-) matter is the most important in the β-stable nucleon + lepton matter. The balance processes for the (n, p, e^-) system are the weak reactions

$$n \longrightarrow p + e^- + \bar{\nu_e} \ , \tag{18}$$

and

$$p + e^- \longrightarrow n + \nu_e \ . \tag{19}$$

The chemical potential equilibrium condition for the (n, p, e^-) system can be written as

$$\mu_e = \mu_n - \mu_p \ . \tag{20}$$

The charge neutrality condition is

$$\rho_e = \rho_p \ , \tag{21}$$

where the electron density ρ_e in the ultrarelativistic limit for non-interacting electrons can be denoted as a function of electron chemical potential

$$\rho_e = \frac{1}{3\pi^2}\mu_e^3 \ . \tag{22}$$

The charge neutrality condition can be rewritten

$$3\pi^2\rho X_p - [4E_{\text{sym}}(\rho)(1-2X_p)]^3 = 0 \ , \tag{23}$$

where $X_p = Z/A = \rho_p/\rho$ is the proton fraction and the asymmetry parameter $\alpha = 1 - 2X_p$. The X_p can be obtained by solving eq. (23). The obtained X_p for the three different scaling parameters y is presented inside fig. 5 as a function of the baryon density. The results show that X_p increases with increasing baryon density for a fixed y and increases with increasing y for a fixed density. We note that in all cases the critical proton fraction value $X_p = 1/9$ to have direct $URCA$ processes [22] is reached at densities as low as about $2\rho_0$. This implies that direct URCA processes are possible also for low mass neutron stars, where in fact the observed cooling rate appears much slower than in higher mass stars. However, we like to note that the cooling rate in the lighter neutron stars is also hindered by a more efficient ${}^1S_0$ proton pairing, as recently shown in ref. [23].

The EOS for β-stable $n + p + e$ (npe) matter at $T = 0$ can be estimated by using the obtained values of X_p.

6 Neutron star structure

For a first investigation of the implications of the present EOS in the neutron star physics we assume a simple nucleonic model, also neglecting the effects of rotational motion. We will then compare our results with more elaborated many-body theories, within the same nucleonic picture.

The structure of neutron stars can be calculated by integrating the Tolman Oppenheimer Volkoff (TOV) equation [24]

$$\frac{\mathrm{d}P(r)}{\mathrm{d}r} = -\frac{G[\epsilon(r) + P(r)][M_{\text{s}}(r) + 4\pi r^3 P(r)]}{r^2[1 - 2GM_{\text{s}}(r)/r]} \ , \tag{24}$$

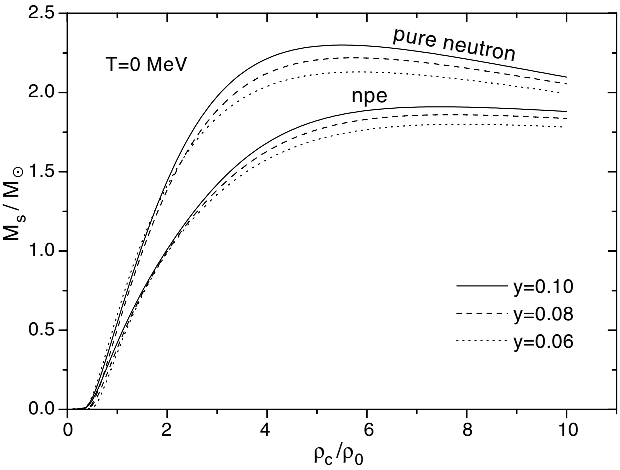

Fig. 6. Comparison between the pure neutron and the β-stable (npe) matter for the ratio of the neutron star mass to the solar mass as a function of the ratio of central density of the star to the saturation density of nuclear matter at $T = 0\,\text{MeV}$ by different parameter y sets.

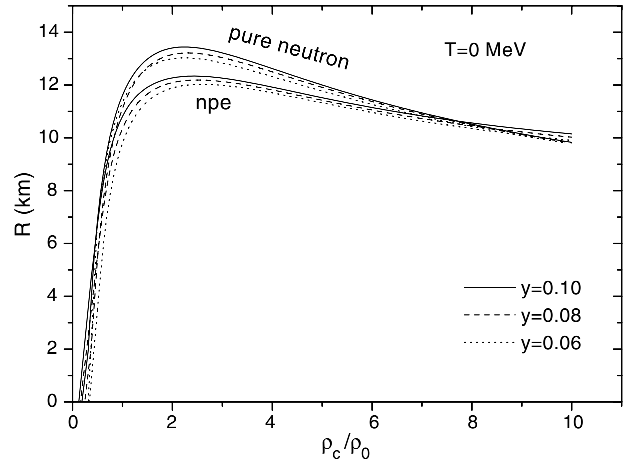

Fig. 7. Comparison between the pure neutron and the β-stable (npe) matter for the radius of the neutron star as a function of the ratio of central density of the star to the saturation density of nuclear matter at $T = 0\,\text{MeV}$ by different parameter y sets.

and

$$\frac{\mathrm{d}M_\mathrm{s}(r)}{\mathrm{d}r} = 4\pi r^2 \epsilon(r) \ , \tag{25}$$

where $M_\mathrm{s}(r)$ is the mass of the star inside the radial coordinate r, and G is the gravitational constant. The radius R of the neutron star is defined by the zero-pressure equilibrium condition

$$P(R) = 0 \ , \tag{26}$$

and the total mass of the neutron star is given by

$$M_\mathrm{s}(R) = \int_0^R \mathrm{d}r 4\pi r^2 \epsilon(r) \ . \tag{27}$$

The properties of neutron star can be studied from eqs. (24)-(27). Based on the above-discussed EOS we have solved the TOV equation to investigate the sensitivity of a pure neutron (α=1) and a β-stable (npe) star structure at $T = 0\,\text{MeV}$ to the BR scaling. In order to make the comparison between the pure neutron-star and the β-stable (npe) matter, fig. 6 displays the ratios of the neutron star mass to the solar mass as a function of the ratio of the central density of the star to the saturation density of nuclear matter for different parameter sets at $T = 0\,\text{MeV}$. As expected the masses of the pure neutron and the (npe) stars are nicely sensitive to the scaling parameter y in the high-density region, with larger differences with the increasing of y.

For a pure neutron star we find that the maximum mass ratios $M_\mathrm{s}/M_\odot$ are 2.30, 2.22 and 2.13 for $y = 0.10$, 0.08 and 0.06, respectively, and the corresponding central density ratios ρ_c/ρ_0 are 5.50, 5.75 and 5.81. For the β-stable (npe) case the maximum ratios $M_\mathrm{s}/M_\odot$ are 1.91, 1.86 and 1.80 for $y = 0.10$, 0.08 and 0.06, respectively, with in correspondence ρ_c/ρ_0 values 7.50, 7.69 and 7.94. These results show that the maximum masses of the pure neutron star and the β-stable (npe) matter increase with the increasing of y whereas the central density of the star decreases. The maximum masses of the β-stable (npe) star

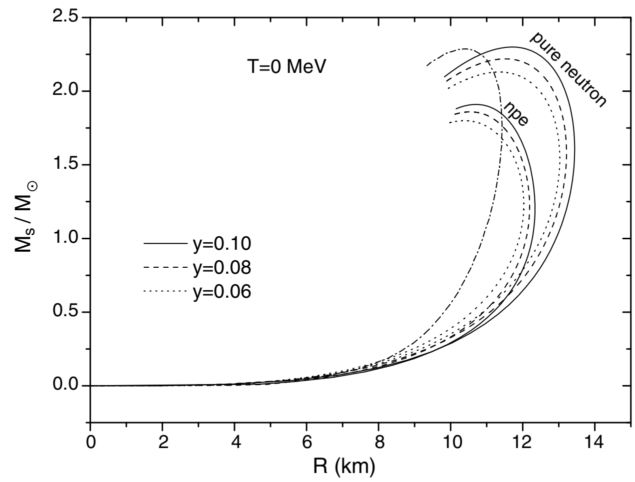

Fig. 8. Comparison between the pure neutron and the β-stable (npe) matter for the ratio of the neutron star mass to the solar mass as a function of the radius of the neutron star at $T = 0\,\text{MeV}$ by different parameter y sets. The dash-dotted line represents the predictions of a non-relativistic BHF calculation for the pure neutron matter case, see text.

for the three different scaling parameters y are less than that of the pure neutron star and the corresponding ratios ρ_c/ρ_0 are larger than that of the pure neutron star. All that is consistent with the fact that for β-stable (npe) matter we have less repulsion due to the relatively larger proton fraction.

The radii of the pure neutron star and the β-stable (npe) matter as a function of the ratio of central density of the star to the saturation density of nuclear matter for different parameter y at $T = 0\,\text{MeV}$ are given in fig. 7. It is seen that the radii of the pure neutron stars and the β-stable (npe) matter increase with increasing y, but the influence of y on the radius is not too large.

Figure 8 shows the ratio of the neutron star mass to the solar mass as a function of the radius of the neutron star for different parameters y at $T = 0\,\text{MeV}$, for the two cases, pure neutron and npe. It is shown that in all cases the mass of a neutron star is not sensitive to y for small radii whereas it becomes sensitive for large ones. The mass of the pure neutron star decreases as y increases for a fixed radius in the range of radii from about 6 to 13 km. Beyond 13 km the mass of the pure neutron star for a fixed y first increases and then backbends passing through the maximum point. The obtained maximum masses of the pure neutron stars are 2.30, 2.22 and $2.13M_\odot$ for $y = 0.10$, 0.08 and 0.06, respectively, and the corresponding radii are 11.71, 11.53 and 11.36 km. The situation for the β-stable (npe) matter is similar with that of the pure neutron case. The mass of the β-stable (npe) star decreases as y increases for a fixed radius in the range of radii from about 5 to 12 km. Beyond 12 km the mass of the β-stable (npe) matter for a fixed y first increases and then backbends passing through the maximum point. The obtained maximum masses of the β-stable (npe) matter are 1.91, 1.86 and $1.80M_\odot$ for $y = 0.10$, 0.08 and 0.06, respectively, and the corresponding radii are 10.69, 10.54 and 10.37 km. It is observed that the radii of both the pure neutron star and the β-stable (npe) matter increase as y increase, and the radius of the pure neutron star for a fixed y is larger than that of the β-stable (npe) matter.

Compared with the possible observations of neutron stars reviewed in ref. [25], it seems that the present model with the BR mass scaling can be used to describe the properties of the neutron stars. In particular we have performed a detailed comparison with completely different microscopic many-body models, of Brueckner-Hartree-Fock (BHF) type, within the same pure nucleonic picture. In fig. 8 we also plot the prediction of a non-relativistic BHF-EOS calculation, including three-body forces [26], for a pure neutron matter case. This comparison could shed some light on the connection between the mass scaling laws and the nucleonic excitations giving rise to the main three-body microscopic forces within the quark sector [27].

We note that the two calculations are showing very similar *Mass-Radius* correlation curves. In particular the maximum masses are very close while the neutron star turns out to be more compact in the BHF case. The values are larger than the observational datum $M_s/M_\odot \approx 1.44$. In fact this is usually assumed as a threshold of the neutron star mass, since it is the most precise observation, but higher values cannot be ruled out. Our result is presumably due to a too crude composition assumed for the star. Indeed we have seen that with inclusion of protons and electrons in beta equilibrium the mass ratio is quenched to a value about two times smaller, with the mechanism described before. An additional inclusion of hyperons is expected to further reduce this value, see ref. [28].

7 Summary and conclusions

The novel and meaningful features of the present model are that the in-medium effects can be largely incorporated in the effective nuclear interaction just by the BR mass scaling procedure. The bare meson masses and meson-nucleon coupling constants adopted in the present calculation are taken from the well-known Bonn potential, which reproduces the experimental phase shifts of the NN scattering and the deuteron binding energy. This procedure allows a separate estimation of other in-medium correlation contributions, in particular of non-linear terms. This is important in order to check the intrinsic consistency of the model.

Our findings show that the BR mass scaling plays an important role in the equation of state of nuclear matter. The obtained results indicate that the present model can reproduce the empirical properties of nuclear matter at zero or finite temperature and make reasonable predictions in different density regions.

Similar effects were already suggested from microscopic many-body calculations [12,13]. We think that it is interesting to show this result within an effective relativistic mean-field framework, which is more physically trasparent and of prompt use for nuclear structure and dynamics problems.

The present model, extended to isospin asymmetric nuclear matter without additional free parameters, is then applied to investigate the properties of the neutron stars and the results are quite reasonable in comparison with different many-body approaches.

We conclude with a general comment. We like to note that that the relative simple functional form of the nuclear EOS obtained from the BR-scaling prescription appears to work amazingly well on a wide range of baryon densities, from zero to roughly five times ρ_0.

We warmly thank H.J. Schulze for the comparison with BHF neutron star structures. This project is supported by the National Natural Science Foundation of China under Grant No. 10275002, the INFN of Italy, and the Major State Basic Research Developing Program with grant No. G2000077400.

References

1. J.D. Walecka, Ann. Phys. (N.Y.) **83**, 491 (1974).
2. B.D. Serot, J.D. Walecka, Adv. Nucl. Phys. **16**, 1 (1986).
3. H. Müller, B.D. Serot, Nucl. Phys. A **606**, 508 (1996).
4. H. Yoshida, H. Sagawa, N. Takigawa, Phys. Rev. C **58**, 2796 (1998).
5. J. Zimanyi, S.A. Moszkowski, Phys. Rev. C **42**, 1416 (1990).
6. G.E. Brown, M. Rho, Phys. Rev. Lett. **66**, 2720 (1991).
7. CERES Collaboration (G. Agakichiev *et al.*), Phys. Rev. Lett. **75**, 1272 (1995).
8. HELIOS-3 Collaboration (M. Masera), Nucl. Phys. **590**, 93c (1995).
9. C. Song, Phys. Rep. **347**, 289 (2001).
10. C. Song, D.P. Min, M. Rho, Phys. Lett. B **424**, 226 (1998).
11. C. Song, G.E. Brown, D.P. Ming, M. Rho, Phys. Rev. C **56**, 2244 (1997).
12. A.B. Santra, U. Lombardo, Phys. Rev. C **62**, 018202 (2000).
13. R. Rapp, R. Machleidt, J.W. Durso, G.E. Brown, Phys. Rev. Lett. **82**, 1827 (1999).

14. R. Machleidt, Adv. Nucl. Phys. **19**, 189 (1989).
15. R.J. Furnstahl, J.J. Rusnak, B.D. Serot, Nucl. Phys. A **632**, 607 (1998).
16. M. Baldo, L.S. Ferreira, Phys. Rev. C **59**, 682 (1999).
17. M.Di Toro *et al.*, Prog. Part. Nucl. Phys. **42**, 125 (1999).
18. B. Liu, V. Greco, V. Baran, M. Colonna, M. Di Toro, Phys. Rev. C **65**, 045201 (2002).
19. M. Malheiro, A. Delfino, C.T. Coelho, Phys. Rev. C **58**, 426 (1998).
20. Guo Hua, B. Liu, M. Di Toro, Phys. Rev. C **62**, 035203 (2000).
21. W.D. Myers, W.J. Swiatecki, Ann. Phys. (N.Y.) **55**, 186 (1969).
22. J.M. Lattimer, C.J. Pethick, M. Prakash, P. Haensel, Phys. Rev. Lett. **66**, 2701 (1991).
23. W. Zuo, Z.H. Li, G.C. Lu, J.Q. Li, W. Scheid, U. Lombardo, H.J. Schulze, C.W. Shen, nucl-th/0403026.
24. R.C. Tolman, Phys. Rev. **55**, 364 (1939); J.R. Oppenheimer, G.M. Volkoff, Phys. Rev. **55**, 374 (1939).
25. G. Baym, Nucl. Phys. A **590**, 233c (1995).
26. X.R. Zhou, G.F. Burgio, U. Lombardo, H.J. Schulze, W. Zuo, Phys. Rev. C **69**, 018801 (2004).
27. K. Saito, K. Tsushima, A.W. Thomas, Phys. Rev. C **55**, 2637 (1997).
28. M. Baldo, G.F. Burgio, H.J. Schulze, Phys. Rev. C **61**, 055801 (2000).